ELSEVIER

Materials Science and Engineering 294–296 (2000) 761–764

MATERIALS SCIENCE & ENGINEERING A

www.elsevier.com/locate/msea

Plastic properties of icosahedral Al–Pd–Mn single quasicrystals

M. Bartsch [a,*], B. Geyer [a], D. Häussler [a], M. Feuerbacher [b], K. Urban [b], U. Messerschmidt [a]

[a] *Max-Planck-Institut für Mikrostrukturphysik, Weinberg 2, Halle/Saale D-06120, Germany*
[b] *Institut für Festkörperforschung, Forschungszentrum Jülich GmbH, Jülich D-52425, Germany*

Received 2 September 1999; accepted 27 October 1999

Abstract

Plastic deformation properties of icosahedral Al–Pd–Mn single quasicrystals have been measured over a wide range of temperature in constant strain rate experiments including stress relaxation tests. The properties are different in the low and high-temperature ranges. At low temperatures, the deformation is controlled by the lattice friction of the gliding dislocations and a very effective work-hardening mechanism. At high temperatures, the deformation properties are discussed in terms of recovery-controlled plastic deformation. © 2000 Elsevier Science B.V. All rights reserved.

Keywords: Icosahedral quasicrystals; Plastic deformation; Stress relaxation; Work-hardening; Recovery

1. Introduction

In the last years, the properties of the plastic deformation of icosahedral single quasicrystals have been investigated by macroscopic compression tests [1–5], transmission electron microscopy of the deformation induced dislocation structure [6,7] and by in situ deformation in a high-voltage electron microscope [8]. In the temperature range between 630 and 830°C, the material is very ductile [1–5]. Recently, plastic deformation of up to about 0.5% plastic strain was achieved even down to 500°C revealing a different deformation behaviour. The present paper compares the deformation behaviour of the low temperature range with that before the upper yield point (i.e. in the pre-yield range) at high temperatures in order to characterize the different deformation mechanisms.

2. Results

Macroscopic compression tests have been performed in the high-temperature range as described in [4]. The deformation behaviour is characterized by the changes of the plastic strain rate during stress relaxation tests (r) and the following reloading (l) in plots of $\ln(S\dot{\varepsilon} - \dot{\sigma})$ versus σ, i.e. for $\dot{\varepsilon} = 0$ the ordinate equals the relaxation rate $-\dot{\sigma}$ but a converted strain rate during loading if $\dot{\varepsilon} \neq 0$. In the shown stress–strain curves, the relaxation and reloading events are indicated. S is the elastic stiffness of the sample which is estimated from the slope of the unloading curve.

Below about 630°C, the specimens break in a brittle way at a strain rate of $10^{-5}\,s^{-1}$. However, plastic strains in the order of 0.5% can be achieved by choosing a strain rate of $10^{-6}\,s^{-1}$ and by performing stress relaxation tests before the stress reaches a critical value of fracture [9]. Fig. 1a shows a stress–strain curve taken at 554°C. Above about 600 MPa, a plastic range begins with only small deviations from the elastic line. Two stress relaxation tests r1 and r2 clearly indicate plastic deformation. In Fig. 1b, r1 and r2 are almost parallel, which corresponds to a shift in stress $\Delta\sigma$ at equal relaxation rates. Together with the increment in plastic strain $\Delta\varepsilon_{pl}$ in Fig. 1a, there follows a work-hardening coefficient Θ of about 100 GPa, which is of the order of the elastic stiffness S. Fig. 2 presents the deformation curves at 612°C. The stress–strain curve of Fig. 2a and the first relaxation r1 in Fig. 2b are similar to those at 554°C, but r2 shows a transition to a slower decrease of the relaxation rate with decreasing stress, indicating the action of a second process developing during straining. Stress dip tests, i.e. partial unloading during relaxation tests were performed in order to separate time and strain dependent processes of the dynamic deformation parameters indicated in Figs. 1 and 2 as r1d. In both figures, the transition between r1d and r2 during loading is demonstrated by the reloading curves l2 if $\dot{\varepsilon} \neq 0$. These curves start at the end of the relaxation curves of r1d and lead to the beginning of r2.

* Corresponding author. Tel.: +49-345-5582-50; fax: +49-345-5511-223.
E-mail address: mbartsch@mpi-halle.de (M. Bartsch).

0921-5093/00/$ – see front matter © 2000 Elsevier Science B.V. All rights reserved.
PII: S0921-5093(00)01108-4

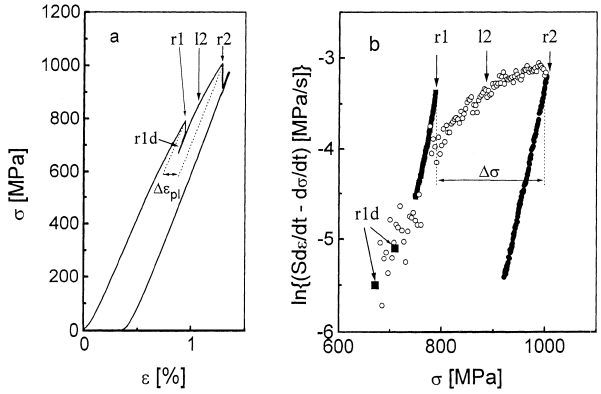

Fig. 1. Deformation curves at 554°C at a total strain rate of 10^{-6}/s. (a) Stress–strain curve with stress relaxations. (b) Stress relaxation curves (r1 and r2) with dip tests (r1d) and reloading curve (l2).

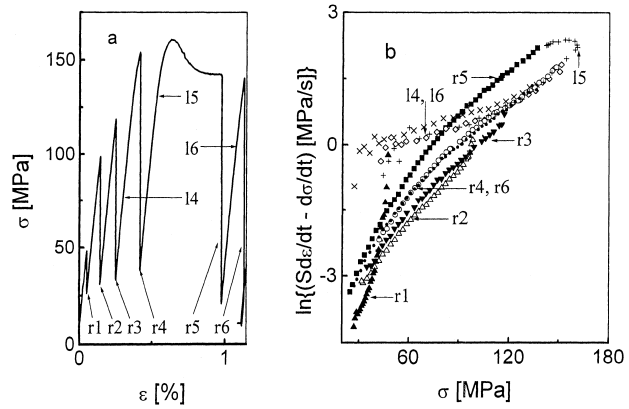

Fig. 3. Pre-yield deformation behaviour at 815°C at a total strain rate of 10^{-4}/s. (a) Stress–strain curve with stress relaxations (r1–r6). (b) Stress relaxation curves in the pre-yield range (r1–r4) and from steady-state deformation (r5), repeated relaxation (r6) and reloading curves (l4–l6).

At low temperatures, if strong work-hardening occurs, the dip tests yield a higher relaxation rate at the same stress than that occurring during continuous relaxation. This shows that work-hardening takes place also during the relaxation tests. In order to estimate the true strain rate sensitivity of the flow stress r, the values $r_{ex} = \Delta\sigma/\Delta \ln \dot{\varepsilon}_{pl} = \Delta\sigma/\Delta \ln(-\dot{\sigma})$ measured from the slope of the relaxation curves have to be corrected for work-hardening according to

$$r = r_{ex}\left(1 + \frac{\Theta}{S}\right) \quad (1)$$

As at low temperatures Θ is of the order of magnitude of S, the corrected values of r are about twice the measured ones and become about 70 MPa as estimated from Figs. 1b and 2b. These values are smaller than those estimated at higher temperatures. Respective activation volumes are given in [10].

In order to compare the deformation properties at low and high temperatures, the pre-yield range of a typical deformation curve is shown in Fig. 3, taken at 815°C and at the higher strain rate of $10^{-4}\,s^{-1}$. The stress–strain curve in Fig. 3a shows a yield drop before a steady-state stress is reached. The latter is characteristic of the high-temperature range. Yield drops occur after the first loading as well as after stress-relaxation tests, unloading and during strain rate cycling experiments, respectively. The relaxation curve r5 in Fig. 3b, starting from the steady-state stress level, exhibits the shape characteristic of the high-temperature deformation (e.g. [2–4]). Repeated relaxations like r6, i.e. relaxation tests starting from the stress level of an original relaxation like r5 without passing the yield drop, show lower relaxation rates than the original relaxation curves [4]. The shape of these two stress relaxation curves (r5 and r6 in Fig. 3b), characteristic of high temperatures, with a low slope from the beginning, remains constant after steady-state plastic deformation is reached independent of the value of the strain as long as the steady-state stress level remains constant. Stress relaxations in the pre-yield range indicate plastic deformation even at low stresses. The loading curves l4–l6 in Fig. 3b show an instantaneous transition of the plastic strain rate from the end of the previous relaxation to a value of about 10% of the total strain rate. Afterwards the strain rate increases with increasing stress, first weakly until it reaches that of the repeated relaxation curve. Above this point, if the curve (l5) proceeds through the yield point, the plastic strain rate increases remarkably. If stress relaxation tests are started at stresses below this point the relaxation curves begin with a steep drop of the relaxation rate (r1–r3 in Fig. 3b) with a low strain rate sensitivity of the flow stress. The stress difference between two of these starting points, about 50 MPa between r1 and r2, is caused by dominating work-hardening with similar high values of Θ as at low temperatures. The first steep drop of the relaxation rate is followed by a part with a smooth change of the relaxation rate with decreasing stress (especially r2 and r3 in Fig. 3b), following the trace of the repeated relaxation curve (r4 and r6). The same plastic properties described for the pre-yield deformation occur also during reloading from a well-relaxed state at higher strains.

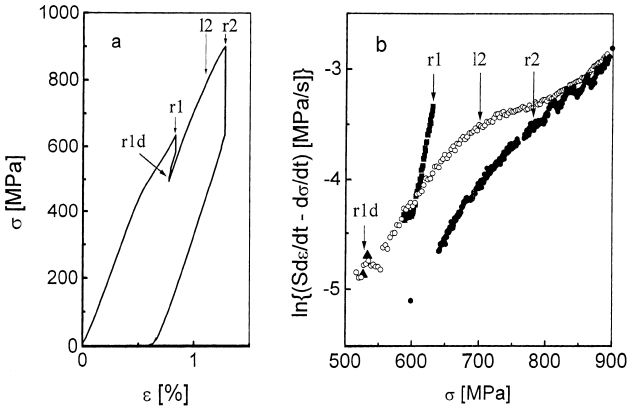

Fig. 2. Deformation properties at 612°C at a total strain rate of 10^{-6}/s. (a) Stress–strain curve with stress relaxations. (b) Stress relaxation curves (r1 and r2) with dip tests (r1d) and reloading curve (l2).

3. Discussion

The deformation properties of Al–Pd–Mn quasicrystals can be summarized as follows. At low temperatures, strong work-hardening leads to very high values of the flow stress. The strain rate sensitivity estimated from stress-relaxation tests has to be corrected for work-hardening. The strong increase of the strain rate sensitivity with decreasing temperature, which was found for the high-temperature range [4], does not continue at low temperatures although the values are still relatively high compared to other materials. At high temperatures, recovery processes prevent the flow stress to increase to high values leading to the well-known rapid decrease of the flow stress with increasing temperature. Besides, transient effects occur as, e.g. the yield drop effects reflecting the differences between original and repeated relaxation curves as well as the transient relaxation behaviour in the pre-yield range after long-time relaxations. In the following, it will be tried to interpret these observations.

At low temperatures, only part of the total flow stress relaxes, which builds up by work-hardening, indicating that the remaining part should be of athermal nature. The relaxing part is certainly controlled by the lattice friction stress of dislocation glide so that the strain rate sensitivity measured at low temperatures is characteristic of the friction mechanism, as discussed in [10].

In order to explain the internal stress the interaction between non-parallel dislocations has to be considered because of the great number of almost equivalent slip systems in quasicrystals. Generally, the athermal part of the flow stress σ_i can be described by the cutting of forest dislocations as well as by the long-range elastic interaction of almost parallel dislocations. The stress components of both mechanisms depend on the mutual distance l between the dislocations resulting in a square root dependence on the dislocation density ρ [11,12]

$$\sigma_i = \alpha \mu b \rho^{1/2} / m_s, \tag{2}$$

where α is a numerical factor near 0.5 for both mechanisms, μ the shear modulus (68 GPa at 610°C), b the length of the Burgers vector in physical space (most frequent value b=0.183 nm, e.g. [6]), and m_s is the orientation factor ($m_s \cong 0.4$). In a simple cube model of the dislocation arrangement, the link length l in a dislocation network is related to ρ by

$$l \cong \left(\frac{3}{\rho}\right)^{1/2} \tag{3}$$

Up to now, the athermal component of the flow stress of quasicrystals has been discussed in terms of the interaction between parallel dislocations, i.e. Taylor hardening [11]. Single values of ρ for the deformation at 610°C in a region of a homogeneous distribution of dislocations and one inside a slip band of 10^{12} and $1.3\times10^{13}\,m^{-2}$ are given in [10]. The latter value yields $\sigma_i \cong 56$ MPa which is too low in order to explain the measured flow stress contribution of the order of 500 MPa, even if a similar additional contribution due to dislocation cutting is taken into account. Thus, dislocation densities which are two orders of magnitude higher than those in the slip bands are necessary to explain the measured high flow stress. Such high dislocation densities are quite unrealistic. This means that cutting the dislocation forest also fails in explaining the high stresses building up by work-hardening during the low-temperature deformation. At present, it can only be speculated about this very effective hardening mechanism. Possible mechanisms are the production of a high concentration of debris or even point defects by jog-dragging or the cutting of phason layers formed on other slip systems. There is no experimental evidence of these models, yet.

The essential difference between the high-temperature and low-temperature ranges seems to be that recovery processes control the deformation at high temperatures. In this respect, the steady-state deformation of quasicrystals does not seem to differ from the creep deformation of other high-temperature materials. For the high-temperature deformation of metals, usually models of link lengths in a dislocation network are being discussed (e.g. [13,14]). The generation of new dislocations leads to the formation of new links and thus to a reduction in the link length connected with work-hardening while the annihilation of links by climb causes recovery. After some strain, a dynamic equilibrium may form. Such a model is consistent with the dislocation structure observed in a specimen from [7] deformed at 730°C and imaged in a high-voltage electron microscope to show the spatial arrangement of the dislocations. They form many nodes with link lengths between them of about 300 nm. This length corresponds to the dislocation densities measured in [7] by using Eq. (3).

According to [7], the dislocation density recovers down to about 40% of its initial value after annealing for about 30 min at the deformation temperature of 730°C. Later on, it remains constant. This state should correspond to the fully relaxed state at the end of the relaxation curves, e.g. like r5, when most of the work-hardening is recovered. Due to the square root dependence of σ on ρ, the difference in the flow stresses between the steady state and the fully relaxed state following from the dislocation densities of [7] should amount to a factor of about 1.6. However, in practice it is 3.5, i.e. the ratio in ρ necessary to explain the flow stress difference should be about 12 instead of 2.5 as measured. Above, it has been discussed that the flow stress at low-temperatures can hardly be explained solely by the change of the dislocation density. Also at high temperatures, the specimens work-harden before the yield point is reached [4,5] so that other mechanisms should operate also at high temperatures. As they are concerned with dislocation debris or other thermally unstable defects, the respective flow stress component may recover much faster and more completely than it

is possible for dislocations. This may explain some of the dynamic features shown in Fig. 3b.

If the specimen is quickly reloaded after a long-time relaxation to an intermediate stress and then relaxed again like r1 in Fig. 1a, the relaxation curve starts with a steep drop of the stress relaxation rate. The starting slope of this curve represents the strain rate sensitivity of the dislocation lattice friction rather than that of a relaxation curve starting from the steady-state deformation. The main process during the first loading is the work-hardening, resulting in a loading curve almost parallel to the stress axis followed by a part just before the macroscopic flow stress is reached controlled by the competition between work-hardening and recovery.

4. Conclusions

- Below about 630°C, the specimens exhibit a strong work-hardening, which cannot be explained by simple models of long-range dislocation interactions alone. In this range, the strain rate sensitivity should characterise the dislocation lattice friction mechanism.
- Above about 630°C, the steady-state deformation can be described by the formation and recovery of deformation-induced defects.
- At high temperatures, the parameters of the lattice friction mechanism can only be determined from the steep parts of the relaxation curves occurring after partial reloading from the well-relaxed state.

Acknowledgements

The authors thank the Deutsche Forschungsgemeinschaft for financial support.

References

[1] M. Wollgarten, M. Beyss, K. Urban, H. Liebertz, U. Köster, Phys. Rev. Lett. 71 (1993) 549.
[2] M. Feuerbacher, B. Baufeld, R. Rosenfeld, M. Bartsch, G. Hanke, M. Beyss, M. Wollgarten, U. Messerschmidt, K. Urban, Phil. Mag. Lett. 71 (1995) 91.
[3] D. Brunner, D. Plachke, H.D. Carstanjen, Mater. Sci. Eng. A 153/154 (1997) 310.
[4] B. Geyer, M. Bartsch, M. Feuerbacher, K. Urban, U. Messerschmidt, Phil. Mag. A 80 (2000) 1151.
[5] U. Messerschmidt, M. Bartsch, B. Geyer, M. Feuerbacher, K. Urban, Phil. Mag. A 80 (2000) 1165.
[6] M. Feuerbacher, C. Metzmacher, M. Wollgarten, K. Urban, B. Baufeld, M. Bartsch, U. Messerschmidt, Mater. Sci. Eng. A 233 (1997) 103.
[7] P. Schall, M. Feuerbacher, M. Bartsch, U. Messerschmidt, K. Urban, Phil. Mag. Lett. 79 (1999) 785.
[8] M. Wollgarten, M. Bartsch, U. Messerschmidt, M. Feuerbacher, R. Rosenfeld, M. Beyss, K. Urban, Phil. Mag. Lett. 71 (1995) 99.
[9] U. Messerschmidt, B. Geyer, M. Bartsch, M. Feuerbacher, K. Urban, Mater. Res. Soc. Symp. Proc. 552 (1999) 319.
[10] U. Messerschmidt, D. Häussler, M. Bartsch, B. Geyer, M. Feuerbacher, K. Urban, Mater. Sci. Eng. A. 294–296 (2000) 757–760.
[11] G.I. Taylor, Proc. R. Soc. 145 (1934) 362.
[12] F.R. Nabarro, Z.S. Basinski, D.B. Holt, Adv. Phys. 13 (1964) 193–323.
[13] H.E. Evans, G. Knowles, Acta Metall. 25 (1977) 963.
[14] B. Burton, Phil. Mag. A 45 (1982) 657.